processes

MDPI

Article

Optimising Batch Sorption: Effect of Mixing Speed and Reactor Design on Wastewater Treatment Kinetics and Efficiency

Anita Bašić [1], Mario Nikola Mužek [2], Željko Penga [3] and Sandra Svilović [1,*]

[1] Department of Chemical Engineering, Faculty of Chemistry and Technology, University of Split, Ruđera Boškovića 35, 21000 Split, Croatia; abasic@ktf-split.hr
[2] Department of Inorganic Technology, Faculty of Chemistry and Technology, University of Split, Ruđera Boškovića 35, 21000 Split, Croatia; muky@ktf-split.hr
[3] Department of Mechanical Engineering and Naval Architecture, Faculty of Electrical Engineering, Mechanical Engineering and Naval Architecture, University of Split, Ruđera Boškovića 32, 21000 Split, Croatia; zpenga@fesb.hr
* Correspondence: sandra@ktf-split.hr

Abstract: The batch sorption process is used to remove various species from wastewater and can be optimised by selecting adequate process parameters and reactor geometry. As sorption is a heterogeneous process, achieving the desired process outcomes in a batch reactor relies heavily on establishing conditions in which the influence of interphase diffusion is minimised while keeping the efficiency and cost of the process at acceptable values. These conditions can be managed by the selection of appropriate reactor geometries and mixing speed through examination of their influence on the sorption yield and cost. The relationship between mixing speed and power consumption is important, as excessive mixing can lead to increased energy costs without proportional gains in sorption kinetics and efficiency. For these reasons, the effect of reactor geometry and mixing speed on copper sorption kinetics, efficiency, and energy consumption was studied. The Ritchie model and Mixed surface reaction and diffusion-controlled sorption kinetic model were employed for the kinetic study. CFD simulations were carried out to identify optimal designs that enhance process efficiency and reduce energy consumption. Data obtained indicate that the sorption process generally follows second-order kinetics. Results demonstrate that sorption can be effectively conducted at impeller speeds lower than the critical suspension speed (N_{JS}), achieving almost equal removal efficiencies (after 30 min) while reducing energy consumption. From the perspective of energy consumption, reactors without baffles are a significantly better solution than baffled reactors, especially when using a PBT impeller. From a kinetic standpoint, better results are achieved at the highest N/N_{JS} or N_{JS}. In baffled reactors, considering both power consumption and process duration, the SBT impeller emerges as the most efficient choice. Considering the compromises between power consumption and process duration the choice of reactor geometry and specific operating conditions should align with process priorities, such as energy savings through lower power consumption or reduced mixing time. FTIR spectra did not reveal the differences in the zeolite structure after the sorption process occurred.

Keywords: sorption kinetics; synthetic zeolite; copper ions; reactor design; CFD; FTIR

check for updates

Academic Editors: Miguel Andrés Peluso and María Victoria Gallegos

Received: 7 January 2025
Revised: 24 February 2025
Accepted: 26 February 2025
Published: 28 February 2025

Citation: Bašić, A.; Mužek, M.N.; Penga, Ž.; Svilović, S. Optimising Batch Sorption: Effect of Mixing Speed and Reactor Design on Wastewater Treatment Kinetics and Efficiency. *Processes* **2025**, *13*, 712. https://doi.org/10.3390/pr13030712

Copyright: © 2025 by the authors. Licensee MDPI, Basel, Switzerland. This article is an open access article distributed under the terms and conditions of the Creative Commons Attribution (CC BY) license (https://creativecommons.org/licenses/by/4.0/).

1. Introduction

The protection and conservation of water resources and ecosystems depends, to a large extent, on the effective removal of pollutants from wastewater before it is discharged

into the environment [1,2]. Industrial wastewater typically contains heavy metals that pose a significant risk to ecosystems and human health due to their toxicity, bioaccumulation potential, and persistence in the environment [2]. When heavy metals enter natural waters, they can accumulate in aquatic organisms, leading to bioaccumulation and biomagnification throughout the food chain, threatening biodiversity and disrupting the stability of ecosystems. In addition, inadequately treated wastewater can leach into the groundwater and jeopardise the health of the surrounding population. Conventional methods of heavy metal removal (chemical precipitation, lime coagulation, membrane filtration, solvent extraction, oxidation, and reduction, etc.) often require significant energy and chemical inputs and can generate secondary pollutants. Among the many different methods that have been proposed for wastewater treatment, sorption has emerged as a successful and effective method [2]. This can be attributed to the reason that it is not only easy to use and effective but also has the ability to eliminate a wide range of pollutants [3]. Sorption could also be cost-effective depending on the selected sorbent and the conditions under which the process is carried out. In a batch sorption process, several key parameters, such as sorbent type, contaminant properties and quantity, reaction conditions, and reactor geometry significantly influence the efficiency and cost of contaminant removal from wastewater. Among the various sorbents investigated, zeolites have proven to be promising candidates due to their high sorption capacity, selectivity, and structural resilience. Zeolites have a well-defined pore structure, a large surface area, and favourable sorption properties. They are particularly effective in removing a variety of pollutants from aqueous solutions, including heavy metals and organic compounds [4]. Their selective affinity for metal ions and their regenerative capacity emphasise their suitability as a reliable and efficient material for wastewater treatment [5]. According to the literature, the NaX zeolite, used as a sorbent in this work, can be reused at least three times and still retains its sorption performance [6,7].

As sorption processes are heterogeneous processes in which the solid phase is involved in mass transfer and reaction, one of the goals of sorption process optimisation is to a) maximise the surface area of the solid particles for reaction or mass transport and b) to reduce boundary layer thickness around sorbent particle [8,9].

Maximising the interface between the two phases to enhance the transport phenomenon is often achieved by operating the mixing process at the critical impeller speed, N_{JS}, i.e., the speed required to fully suspend the particles [10]. Although operating under N_{JS} is usually most advantageous, some processes operate at $N > N_{JS}$ while at the same time, some industrial reactors normally operate at $N < N_{JS}$ [8,10]. Several authors assert that operating at N_{JS} can lead to unnecessarily high power usage as the suspension of the last fillet pieces of the solid particles requires a significant increase in impeller speed and thus increased energy consumption [10]. It is proposed to use the so-called N_{SS} (sufficient suspension impeller speed) which is defined as the speed at which 98% of the solid is suspended [10]. The average difference between these two speeds is about 30% [10]. However, it is not always necessary to find the speed at which 98% of the solids are suspended. For example, for the sorption process, it could be proposed that N_{SS} is the lowest mixing speed for carrying out the sorption process at which there is no effect of external film diffusion and the removal efficiency is almost equal to the one at N_{JS}. Applying this definition to previous research, in which the effect of mixing speed regarding N_{JS} was studied, then for a propeller agitator (D/d_T = 0.46, C/H = 0.33) N_{SS} is expected to be equal to N/N_{JS} = 0.9. For a Pitch Blade Turbine—PBT (D/d_T = 0.57) its value depends on the impeller position and varies between 0.7 and 0.8 N/N_{JS} [11,12]. As for using a speed higher than N_{JS}, previous research obtained for propeller agitators shows that an increase in impeller speed beyond N_{JS} enhances the removal efficiency of the process, has a negligible influence on rate constant, and has a negative effect on power consumption [11]. When using a

Straight Blade Turbine—SBT, increasing impeller speed up to N/N_{JS} = 1.2 has a positive effect on the kinetics. However, a further increase in impeller speed leads to the appearance of aeration and has a negative effect on efficiency and kinetics [13].

Computational Fluid Dynamics—CFD simulations help to improve the design of stirred-tank reactors used in the chemical industry. Researchers can determine the optimal configuration for producing equitable mixing, maximising the rate of reaction, and avoiding stagnant zones by computational modelling of various impeller designs, agitation speeds, and baffle configurations [14]. CFD simulations allow researchers to forecast the impact of parameter alterations (such as impeller design or rotational speed) on power consumption and, through mixing efficiency, the process efficiency as well. Applying CFD simulations, the ideal reactor designs that maximise process efficiency and minimise energy use could be determined [15]. Along with CFD simulations, accurate models of sorption kinetics, which should include rate constants, are required to ensure the lowest operating costs, which according to the literature account for about one-third of the costs associated with operating a water treatment plant [16]. Besides operational cost, kinetics models are needed for the optimisation of design parameters, process duration, and batch reactor dimensions [17].

A wide range of kinetic models can be found in the literature for this purpose. The sorption process can be divided into four successive steps. The first step is bulk transport, the second is film diffusion (diffusion of the solute through the liquid film surrounding the particles), then intraparticle diffusion (diffusion of the solute into the pores of the sorbent), and finally, the surface reaction. The overall rate of the sorption process may be governed by either of these steps or, in certain conditions, by a combination of two steps [18–20]. The two main groups of sorption kinetics models are the diffusion-based models and the reaction-based models. In addition to these two main groups, there is also the Mixed surface reaction and diffusion-controlled adsorption kinetic model (Mixed kinetic model). This model was developed under the assumption that both diffusion and surface reaction control the overall rate of the sorption process [19].

Diffusion-based models are used when the process rate is dependent upon the rate at which components diffuse through the liquid film around the particles or the pores of the particle. The most used external (film) diffusion models and/or internal (particle) diffusion models are the Weber–Morris model, Boyd model, Frusawa and Smith model, Phenomenological internal mass transfer model, etc. [21]. Among reaction-based models, the most used are pseudo-first-order kinetic models, models that are pseudo-second-order kinetic models (Blanchard, Ho), Mixed-order models, the Ritchie model (nth-order), and the Elovich kinetic model [22,23].

The existing studies on sorption mostly focus on investigating how temperature, initial concentration, sorbent dosage, time and randomly selected mixing speed affect the process [24]. There is insufficient research on the influence of reactor geometry and impeller speed on sorption, regarding the influence of the impeller speed that is related to the state of suspension and at the same time provides the simulation of the behaviour in the reactor using CFD.

The novelty of this research is to further enhance understanding of sorption kinetics, efficiency, and energy consumption, primarily focusing on the reactor's geometry, specifically the impacts of the impeller type and baffle presence, and impeller speed i.e., different N/N_{JS} ratios. Transient CFD simulations were conducted using ANSYS Fluent v17.2 to improve understanding of the system's hydrodynamics as simulations using CFD, providing insight into fluid flow, velocity fields, and turbulence, which are essential for optimising processes like batch sorption.

The Ritchie kinetic model and the Mixed kinetic model were employed to simulate experimental kinetic data, with the objective of determining the rate-limiting step and the

process rate, i.e., process duration for different reactor geometry. The final objective is to explore whether optimising reactor geometry and adjusting the mixing intensity can effectively reduce process costs while maintaining process efficiency.

2. Materials and Methods

2.1. Materials and Reagents

The crushed zeolite NaX (Sigma-Aldrich, Merck KgaA, St. Louis, MO, USA) was sieved on a Retsch AS 200 digit laboratory sieve shaker (Retsch GmbH, Haan, Germany) through sieves with different mesh sizes and an amplitude of 2.5 mm. Particles smaller than 0.050 mm were selected for the experiments conducted. A $Cu(NO_3)_2 \cdot 3H_2O$ (Kemika, Zagreb, Croatia) solution with an initial concentration of 7.12 ± 0.09 mmol/dm^3 was prepared by dissolving the corresponding weight of salt in distilled water.

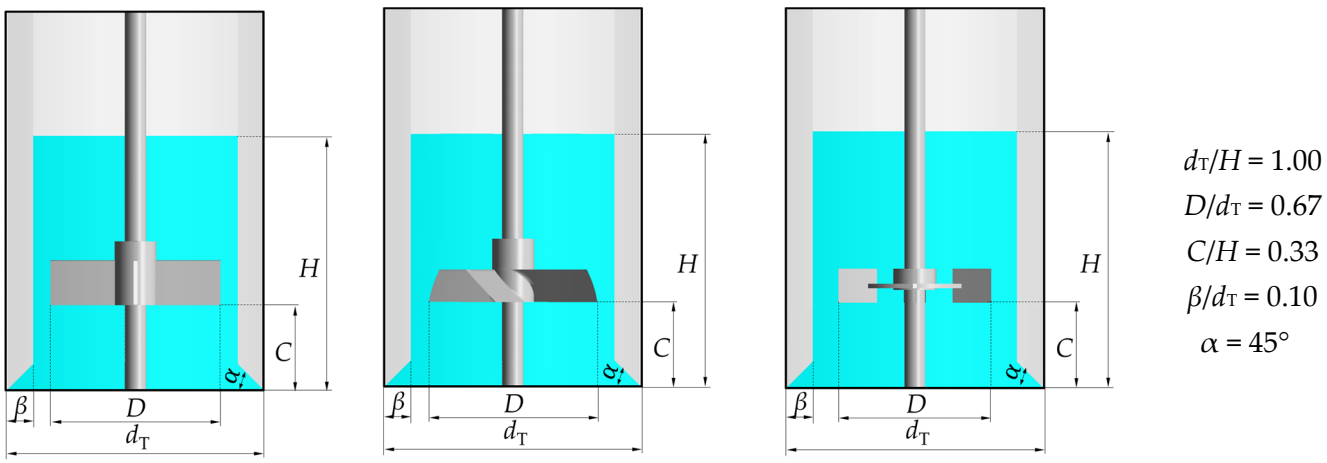
2.2. Instrumentation

The initial concentrations of the copper solutions were checked with the Lambda 25 UV/Vis spectrophotometer from Perkin Elmer (Waltham, MA, USA).

The Universal attenuated total reflectance-Fourier transform infrared spectroscopy (UATR-FTIR) was performed before and after the sorption process, i.e., after saturation with copper ions, to evaluate possible changes in the zeolite NaX due to the presence of heavy metal ions. The spectra were obtained in triplicate on a Perkin Elmer Spectrum Two FTIR spectrometer (Perkin Elmer, MA, USA) equipped with a diamond reflection crystal for collecting spectra by the method of universal attenuated total reflectance, UATR-FTIR at 4000 to 450 cm^{-1} range with a resolution of 4 cm^{-1}.

2.3. Kinetic Experiments and Kinetics Models

All kinetic experiments were carried out in a batch reactor, with each experiment repeated three times. The reactor was made of glass so that the process could be monitored visually. The inner diameter of the reactor was d_T = 0.12 m and the height of the solution, H, was equal to the inner diameter of the reactor ($d_T = H$). When the experiments were carried out in a reactor with baffles, it was equipped with four baffles arranged at a 90° angle around the edge of the vessel (Figure 1). Unbaffled reactors were not presented in the figure, as the same reactors were only used without baffles.



(**a**) Batch reactor with SBT (**b**) Batch reactor with PBT (**c**) Batch reactor with Rushton turbine

Figure 1. Baffled batch reactors with different impellers—design details.

The suspension, 1.3 dm^3 copper solution and 6.5 g zeolite NaX were stirred at a constant temperature (T = 300 K) in a batch reactor. Each batch reactor was equipped with

an impeller. A Straight Blade Turbine impeller (SBT) and a Pitch Blade Turbine impeller (PBT), both with four blades, and a Rushton Turbine (RT), a disc with 6 blades were used. The impeller diameter, D, was 0.08 m and its position, i.e., impellers' off-bottom clearance (C/H) was 0.33.

Firstly, the critical impeller speed, N_{JS}, was determined for all reactor geometries. Mixing was carried out using the IKA® EuroStar 60 Control mixer (IKA-WERKE GMBH & Co. KG, Staufen im Breisgau, Germany), which allows the impeller speed to be regulated and the torque to be measured over the process time. The N_{JS} was determined with a visual method using the Zwietering 1 s criterion [25]. The procedure was explained in detail in previous work [26]. The kinetic experiments were carried out for parameter combinations presented in Table 1.

Table 1. Variable experimental conditions.

Impeller	Baffles	Impeller Speed Ratio N/N_{JS}
SBT	Without	0.75; 1.00; 1.25
	With	
PBT	Without	
	With	
RT	Without	
	With	

The samples were taken from the batch reactor at specific time points, centrifuged and filtered before being analysed with the UV/Vis spectrophotometer. The amount of copper retained on the zeolite during experiments, q_t (mmol/g), and sorption process efficiency after 30 min, R (%), were calculated as follows:

$$q_t = \frac{(c_0 - c_t)\cdot V}{m} \quad (1)$$

$$R = \frac{(c_0 - c_k)}{c_0}\cdot 100 \quad (2)$$

where c_0 is the initial concentration of copper solution (mmol/dm^3), c_t is the concentration of copper solution at time t (mmol/dm^3), V is the volume of solution (dm^3), m is the mass of zeolite (g), and c_k is the concentration of the copper solution at the end of the experiment (mmol/dm^3).

To investigate whether the applied impeller speed N is sufficient to avoid the effects of film diffusion, the kinetic analysis of the obtained experimental data was performed using the Mixed kinetic model and the reaction-based Ritchie model.

The Mixed kinetic model is expressed as [19]:

$$q_t = q_e\cdot\frac{e^{(a\cdot t + b\cdot t^{1/2})} - 1}{u_e\cdot e^{(a\cdot t + b\cdot t^{1/2})} - 1} \quad (3)$$

where: $u_e = 1 - \frac{c_e}{c_0}$, $a = k\cdot c_0\cdot(u_e - 1)$, $b = 2\cdot k\cdot c_0\cdot\psi^{1/2}\cdot(u_e - 1)$, $q_e = \frac{V\cdot c_0\cdot u_e}{m}$, c_e is the concentration at equilibrium (mmol/dm^3), ψ is a parameter that defines the contribution of the diffusion process on the rate of the adsorption (min); if $\psi > 0$ the diffusion affects the kinetics. This model is used when the rates of reaction and diffusion are similar and is not possible to simplify the kinetic model for the overall rate to the model of the slowest process.

The reaction-based model, the Ritchie model, is presented as [27]:

$$\frac{d\theta}{dt} = k_r \cdot (1-\theta)^n \quad (4)$$

where θ is the relative adsorption coverage by the solute; k_r (g/mmol min) is the rate constant of the Ritchie model. After integration Equation (4) for the boundary conditions $\theta = \theta_0$ at $t = t_0$ and $\theta = \theta$ at $t = t$, and n = 2 (assumption: second-order reaction) becomes:

$$q_t = q_e \cdot \left(1 - \frac{1}{1 + k_r \cdot t}\right) \quad (5)$$

where q_e is the amount of copper adsorbed at equilibrium (mmol/g), t is the time (min).

The fitting of the experimental data to the kinetic models was performed with Mathcad (Mathcad Prime 3.0, PTC, Boston, MA, USA) using nonlinear regression.

Transient multiphase computational fluid dynamics simulations of flow in baffled and unbaffled reactors were conducted using the commercial program ANSYS Fluent v17.2 (ANSYS, Canonsburg, PA, USA), and system torques—τ (N m), at the obtained N_{JS}, were calculated. The employed numerical model was the Transition Shear Stress Transport (Transition SST) model, and the methodology is detailed elsewhere [28].

3. Results and Discussion

For a better understanding of the subject matter, the results and discussion are divided into several sections:

- The influence of the impeller type and the presence of baffles in the reactor on the N_{JS}
- Analysis of power consumption at different N/N_{JS} ratios
- The influence and comparison of N/N_{JS} ratios, baffle presence, and impeller type on sorption kinetics and efficiency
- FTIR analysis of zeolite before and after the sorption process.

3.1. The State of Complete Suspension

When a complete suspension is achieved, the maximum surface area of the particles is exposed to the solution for the reaction or transfer processes in the reactor. According to the Zwietering criterion, N_{JS} represents the impeller speed at which all particles are in motion and no solid remains on the reactor bottom for more than 1 s. Figure 2 shows the effects of the impeller type and the presence of baffles on the value of N_{JS}.

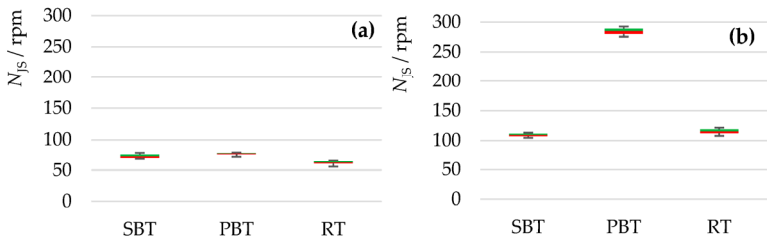


Figure 2. The N_{JS} values in (**a**) unbaffled and (**b**) baffled batch reactors.

The results show that the N_{JS} values are lower and almost the same in a system without baffles for all impellers used.

In a system with baffles the N_{JS} is significantly higher when a PBT impeller is used, while for the other two impellers, the values are lower and similar, but again higher than ones obtained in the unbaffled reactor. It is noteworthy that the aeration was noticed in the baffled reactor equipped with the PBT impeller at speeds higher than 200 rpm. The results obtained are in agreement with the previous results [26,29,30]. Since the fluid flow

developed in the reactor is responsible for the suspension of solids, the results obtained can be clarified by analysing the flow patterns in all the systems.

Figures 3 and 4 present velocities in the stationary frame and vector plots at N_{JS} for different impeller types and reactor systems.

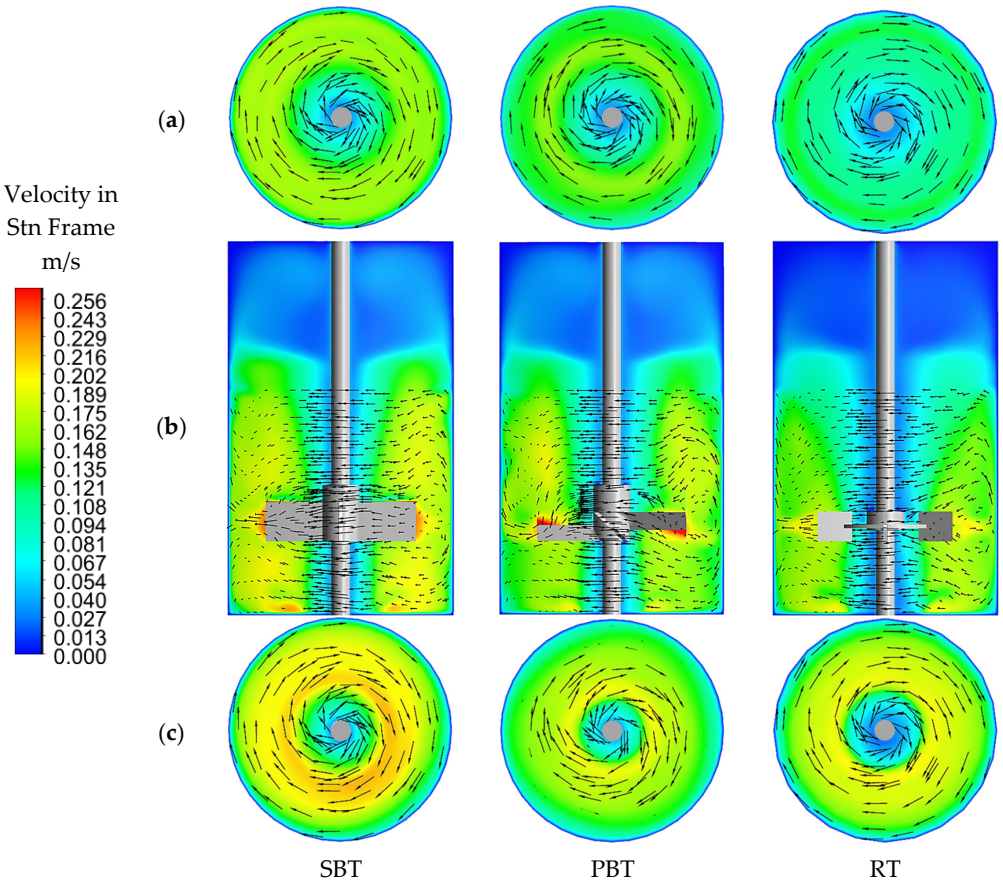


Figure 3. Velocities in the stationary frame and vector plots at N_{JS} in the unbaffled reactors for different impeller types top view at 0.115 m (**a**) and 0.005 m (**c**), and side view (**b**) of the suspension.

It is known that the liquid in a reactor without baffles rotates in a vortex motion [26]. Suspension is divided into a swirling inner region around the shaft and a larger external region with higher velocities. The shape and depth of the vortex formed depend on the impeller speed, the viscosity of the liquid and the reactor geometry, in particular the off-bottom clearance and the diameter of the impeller [31]. In contrast to the bottom of the reactor where a small difference can be observed in velocity in the stationary frame when different impellers are used, the speed distribution and flow in the rest of the reactor do not depend significantly on the impeller type, as can be seen in Figure 3.

In baffled reactors, the SBT impeller and RT impeller generally deflect the flow radially [32,33]. The suspension is discharged from the impeller in a radial direction to the reactor wall, where it splits into two loops differing in intensity and/or extent—one to the bottom of the reactor (lower loop) and the other to the surface (upper loop). The lower loop reaches the bottom of the vessel and keeps the particles in suspension [33]. It can be seen (Figure 4) that the SBT impeller and the RT impeller do not generate the expected flow in the geometries analysed. Inside the reactor with the SBT impeller, an upper flow directed towards the surface and a lower flow directed towards the bottom of the reactor are formed. However, the characteristic "eight" does not form, as the turbulence in the upper right part of the reactor is directed outwards from the shaft towards the reactor wall. It is assumed that the diameter of the impeller, i.e., a high D/d_T ratio causes the unstable flow. The

development of the so-called unstable flow was also observed by Uehara-Nagamine during the investigation of the influence of the off-bottom clearance on the liquid flow generated by SBT [34].

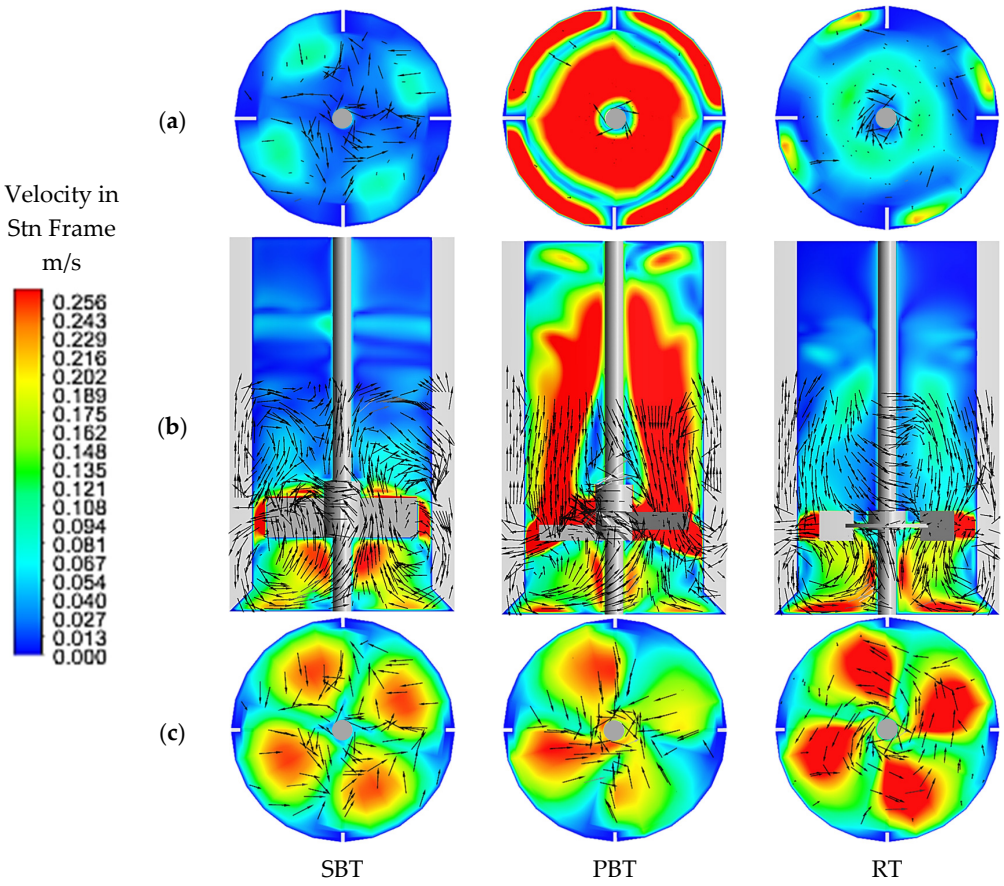


Figure 4. Velocities in the stationary frame and vector plots at N_{JS} in the baffled reactors for different impeller types top view at 0.115 m (**a**) and 0.005 m (**c**), and side view (**b**) of the suspension.

On the other hand, the PBT impeller generally generates an axial flow with a more or less pronounced radial component, i.e., the so-called mixed flow, depending on the off-bottom clearance, the impeller diameter, the blade inclination, and/or the presence of baffles. The PBT impeller generally discharges the liquid to the angle enclosed by the wall and bottom of the tank, from where it then flows to the surface [28,35]. However, in this study due to the proximity of the blades and the baffle/reactor wall, a radial component of the flow is more pronounced. The same observation for a similar geometry (C/H = 0.33, D/d_T = 0.68) was made by Bašić et al. [26]. Kresta et al. observed that the PBT flow field undergoes a transition at a C/D ratio of 0.6, confirming deviations from the characteristic flow due to the geometrical configuration of the reactor and/or the impeller [36]. In the region below the PBT impeller, the velocities are low. At the same time, the velocities in the upper part of the reactor (from the impeller to the surface) are much higher and are accompanied by intensive aeration. The high value of the N_{JS} results from the fact that the lower circuit is responsible for the suspension of the zeolite particles that settle at the bottom of the reactor.

3.2. Power Consumption

The torque on the impeller shaft, τ_e (N cm), was computed by the IKA® EuroStar 60 Control and used to validate a developed computational fluid dynamics model. The

validity of the CFD simulations for all geometries analysed with experimentally computed torque values at N_{JS} can be found in Table 2 (τ_{CFD} stands for the CFD computed torque).

Table 2. Details of the CFD simulations validity for geometries investigated with experimentally computed torque values at N_{JS}.

Impeller	Unbaffled Reactor		Baffled Reactor
SBT	τ_e, N cm	0.1	0.9
	τ_{CFD}, N cm	0.0808	0.7784
PBT	τ_e, N cm	0.1	1.8
	τ_{CFD}, N cm	0.0673	1.6811
RT	τ_e, N cm	0.1	1.2
	τ_{CFD}, N cm	0.0882	1.2549

The CFD computed torque is more precise so it was used to analyse the effect of impeller type and the presence of baffles on power consumption at complete suspension state. The results are presented in Figure 5 and were calculated using the Equation (6):

$$P_{JS} = 2 \cdot \pi \cdot \tau_{CFD} \cdot N_{JS} \quad (6)$$

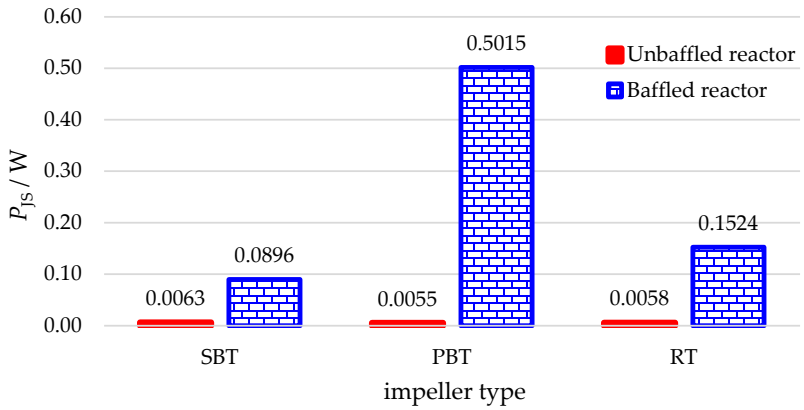


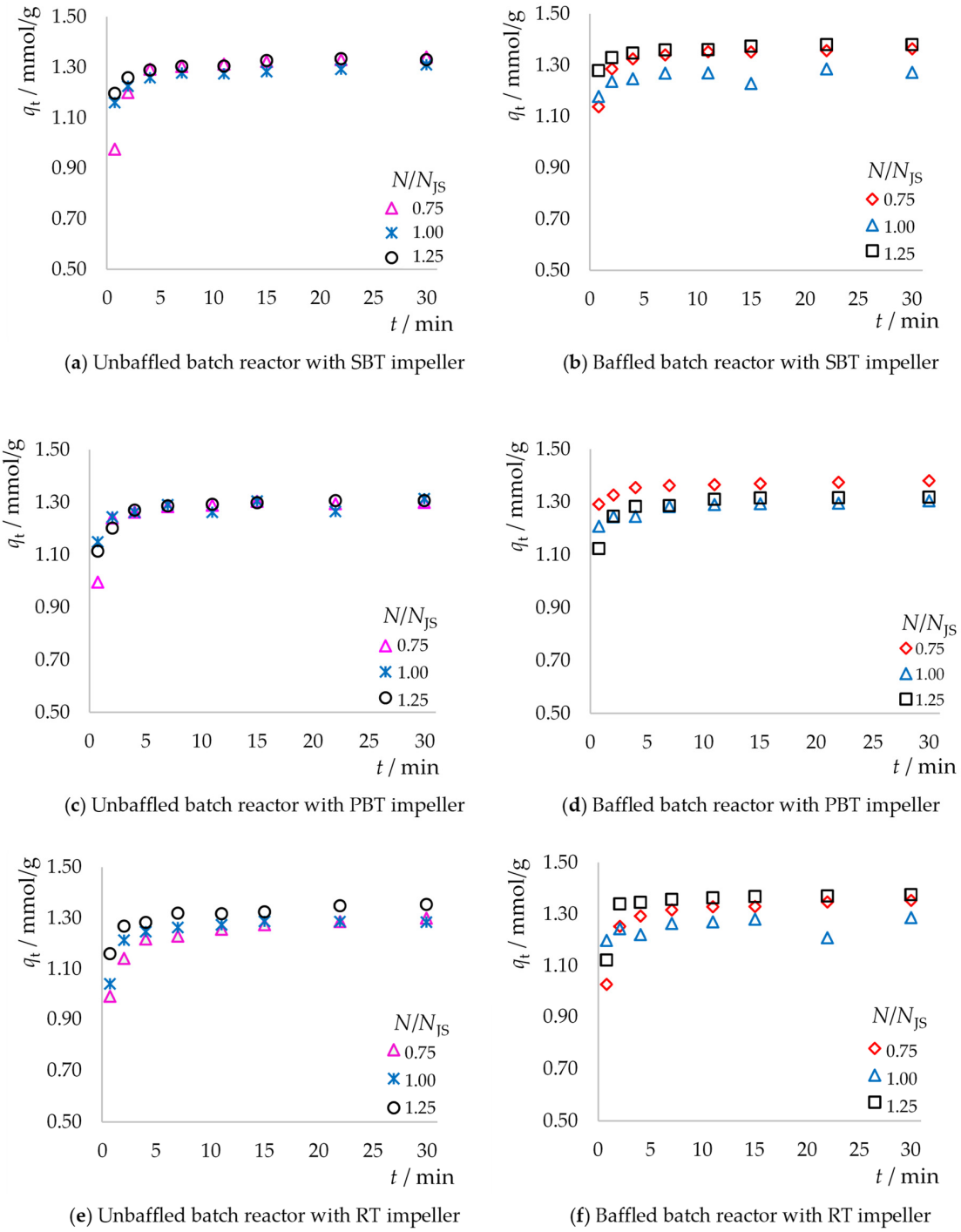
Figure 5. Power consumption at complete suspension state in unbaffled and baffled batch reactor for three different impellers.

Power consumption is higher in a baffled system as it depends on the speed of the impeller and increases as the speed of the impeller increases. It also depends on the torque, which was generally higher in the reactors with baffles, as the baffles provide additional resistance to the liquid flow [26,28]. The highest power consumption is calculated in the reactor with baffles equipped with a PBT impeller, and the lowest in the reactor with the same impeller but without baffles. The lower values of mixing power consumption in the reactor without baffles proved once again that systems without baffles require less energy than those with baffles. The same was observed in the works provided by Bašić et al. for the PBT impeller [26], and Brucato et al. for the RT impeller [37]. The P_{JS} values also show that the presence of aeration increases power consumption.

3.3. Kinetic Experiments

As can be seen in Figure 6, the maximum amount of copper sorbed after 30 min varies slightly depending on the initial concentration (due to the small differences in the prepared solution concentration) and the mixing intensity, which is influenced by the impeller type and the presence of baffles. The experimental kinetic results show that the amount of

copper sorbed increases sharply in the initial phase of the process and then gradually increases until equilibrium is reached for all the hydrodynamic conditions investigated.



(**a**) Unbaffled batch reactor with SBT impeller

(**b**) Baffled batch reactor with SBT impeller

(**c**) Unbaffled batch reactor with PBT impeller

(**d**) Baffled batch reactor with PBT impeller

(**e**) Unbaffled batch reactor with RT impeller

(**f**) Baffled batch reactor with RT impeller

Figure 6. Dependence of copper ions sorption kinetics on impeller type and presence of baffles.

The results presented in Tables 3–5 show that the process studied follows second-order kinetics. The AARD values below 5% show that all the N/N_{JS} ratios are applied to ensure effective mixing that eliminates film resistance. In most cases, ψ equals zero, or its value is slightly higher suggesting that diffusion does not affect the kinetics of copper ions removal on zeolite NaX.

Table 3. Experimental data and parameters of the models applied for SBT impeller.

		Unbaffled Reactor			Baffled Reactor		
Experimental data	N/N_{JS}	0.75	1.00	1.25	0.75	1.00	1.25
	q_{max}, exp (mmol/g)	1.341	1.310	1.330	1.364	1.317	1.381
	u_e, exp	0.939	0.930	0.929	0.944	0.912	0.953
Kinetic model	Parameter						
Ritchie model	q_e (mmol/g)	1.355	1.294	1.330	1.370	1.318	1.375
	k_r (g/mmol min)	3.585	10.947	11.276	6.719	17.927	17.002
	AARD	0.679	0.09	0.591	0.252	0.477	0.417
Mixed kinetic model	$q_e = \frac{V \cdot c_0 \cdot u_e}{m}$ (mmol/g)	1.333	1.282	1.318	1.356	1.309	1.367
	k (dm^3/mmol min)	0.454	1.237	1.291	0.646	1.630	1.708
	ψ (min)	0.000	0.000	0.000	0.018	0.000	0.000
	u_e	0.923	0.910	0.921	0.939	0.907	0.944
	AARD	0.599	0.896	1.011	0.272	0.736	0.745

Table 4. Experimental data and parameters of the models applied for PBT impeller.

		Unbaffled Reactor			Baffled Reactor		
Experimental data	N/N_{JS}	0.75	1.00	1.25	0.75	1.00	1.25
	q_{max}, exp (mmol/g)	1.300	1.314	1.307	1.380	1.304	1.318
	u_e, exp	0.918	0.926	0.919	0.967	0.929	0.926
Kinetic model	Parameter						
Ritchie model	q_e (mmol/g)	1.322	1.297	1.310	1.374	1.293	1.324
	k_r (g/mmol min)	4.535	10.525	7.193	19.464	16.988	7.574
	AARD	1.115	0.946	0.439	0.287	0.700	0.241
Mixed kinetic model	$q_e = \frac{V \cdot c_0 \cdot u_e}{m}$ (mmol/g)	1.302	1.284	1.294	1.368	1.283	1.309
	k (dm^3/mmol min)	0.555	1.102	0.823	1.882	1.606	0.779
	ψ (min)	0.000	0.000	0.000	0.007	0.000	0.000
	u_e	0.920	0.906	0.910	0.958	0.915	0.920
	AARD	0.695	1.119	0.898	0.474	1.123	0.806

The results obtained are presented as changes in mixing speed, power consumption, rate constant and removal efficiency after 30 min depending on the type of impeller for different N/N_{JS} and depending on N/N_{JS} for different types of impellers, Figures 7 and 8. In a reactor without baffles, the type of impeller has no significant effect on N_{JS}, and thus similar N values, for a given N/N_{JS} are used, for all types of impellers. The calculated power consumption also does not vary significantly between impeller types for the same N/N_{JS} ratio. This is a consequence of the flow pattern in unbaffled reactors, which, for the proposed geometry, does not depend on the type of impeller.

In baffled reactors, for SBT and RT impellers, the determined N_{JS} values are approximately the same. Although the N values, used in experiments, for these two types of impellers are close, the power consumption for RT impellers is a bit higher. The difference in power consumption between SBT and RT increases as the N/N_{JS} ratio rises. Ameur et al. also found a slight increase in power consumption for radial impellers with a disk compared to those without one when studying the mixing characteristics of a disk impeller, a radial turbine with six flat blades, and a six-blade Rushton turbine [38]. The highest N/N_{JS} value was determined for the PBT impeller, which also exhibits the highest power consumption.

Table 5. Experimental data and parameters of the models applied for RT impeller.

		Unbaffled Reactor			Baffled Reactor		
Experimental data	N/N_{JS}	0.75	1.00	1.25	0.75	1.00	1.25
	q_{max}, exp (mmol/g)	1.300	1.269	1.354	1.353	1.327	1.375
	u_e, exp	0.924	0.909	0.941	0.936	0.930	0.963
Kinetic model	Parameter						
Ritchie model	q_e (mmol/g)	1.290	1.302	1.342	1.362	1.313	1.391
	k_r (g/mmol min)	4.273	6.091	8.314	4.362	19.987	6.234
	AARD	0.764	1.123	0.625	0.672	0.652	1.036
Mixed kinetic model	$q_e = \frac{V \cdot c_0 \cdot u_e}{m}$ (mmol/g)	1.293	1.285	1.328	1.342	1.305	1.378
	k (dm^3/mmol min)	0.136	0.713	0.970	0.533	1.828	0.793
	ψ (min)	1.882	0.000	0.000	0.000	0.000	0.000
	u_e	0.919	0.920	0.923	0.928	0.914	0.964
	AARD	0.589	1.064	0.992	0.720	0.996	0.829

The trend of the Ritchie rate constant's change depends on the presence of baffles, the type of impeller, and the N/N_{JS} ratio. In general, the presence of baffles has a greater impact than the effect of the impeller type on the rate constant, regardless of the N/N_{JS} ratio. In reactors without baffles, almost identical constant values were obtained for all impellers used at N/N_{JS} = 0.75. As the N/N_{JS} ratio increases, differences in the calculated k_r values rise. In general, the highest k_r values are achieved with the SBT impeller in reactors without baffles. In reactors with baffles, as mentioned previously, the variations in calculated k_r are more significant. The impeller type has a minor impact on k_r at N_{JS}, but both the N/N_{JS} ratio and the impeller type influence the k_r when N/N_{JS} differs from one. The highest k_r value at N/N_{JS} = 0.75 was obtained with a PBT impeller, at N/N_{JS} = 1 with an RT impeller, and at N/N_{JS} = 1.25 with an SBT impeller. The smallest differences in the calculated rate constants were observed for N_{JS}.

In unbaffled reactors, the removal efficiencies after 30 min remain consistent (approximately 92–94%) regardless of the impeller type or N/N_{JS} ratio. This suggests that sufficient suspension was achieved in these experiments. In baffled reactors, the removal efficiency after 30 min is slightly higher under specific conditions (i) PBT impeller at the lowest N/N_{JS} ratio (ii) RT impeller at the highest ratio. From this, it can be concluded that the sorption efficiency remains mostly unaffected by increasing the N/N_{JS} ratio. Considering only sorption efficiency, the process can be effectively conducted at a speed of $0.75N_{JS}$, leading to a reduction in power consumption of at least 43%. At this speed, the unsuspended fillets are quite small and can be considered negligible from a practical perspective, as a significant amount of energy would otherwise be required to suspend these fillets. On the contrary, the rate constant k_r, which correlates with the process duration, is generally highest at N_{JS}. This implies that, for most geometry used, processes operating at N_{JS} minimise process time. Exceptions include the PBT impeller in a baffled batch reactor, where k_r is highest at N/N_{JS} = 0.75. In summary, selecting operational parameters requires balancing power consumption, suspension efficiency, and process time. In this study, N_{JS} offers the most favourable compromise for unbaffled reactor configurations. For baffled reactors, the choice is more complex, except in reactors equipped with a PBT impeller, where lower N/N_{JS} ratios may be advantageous. However, the overall configuration with a PBT impeller is economically inefficient.

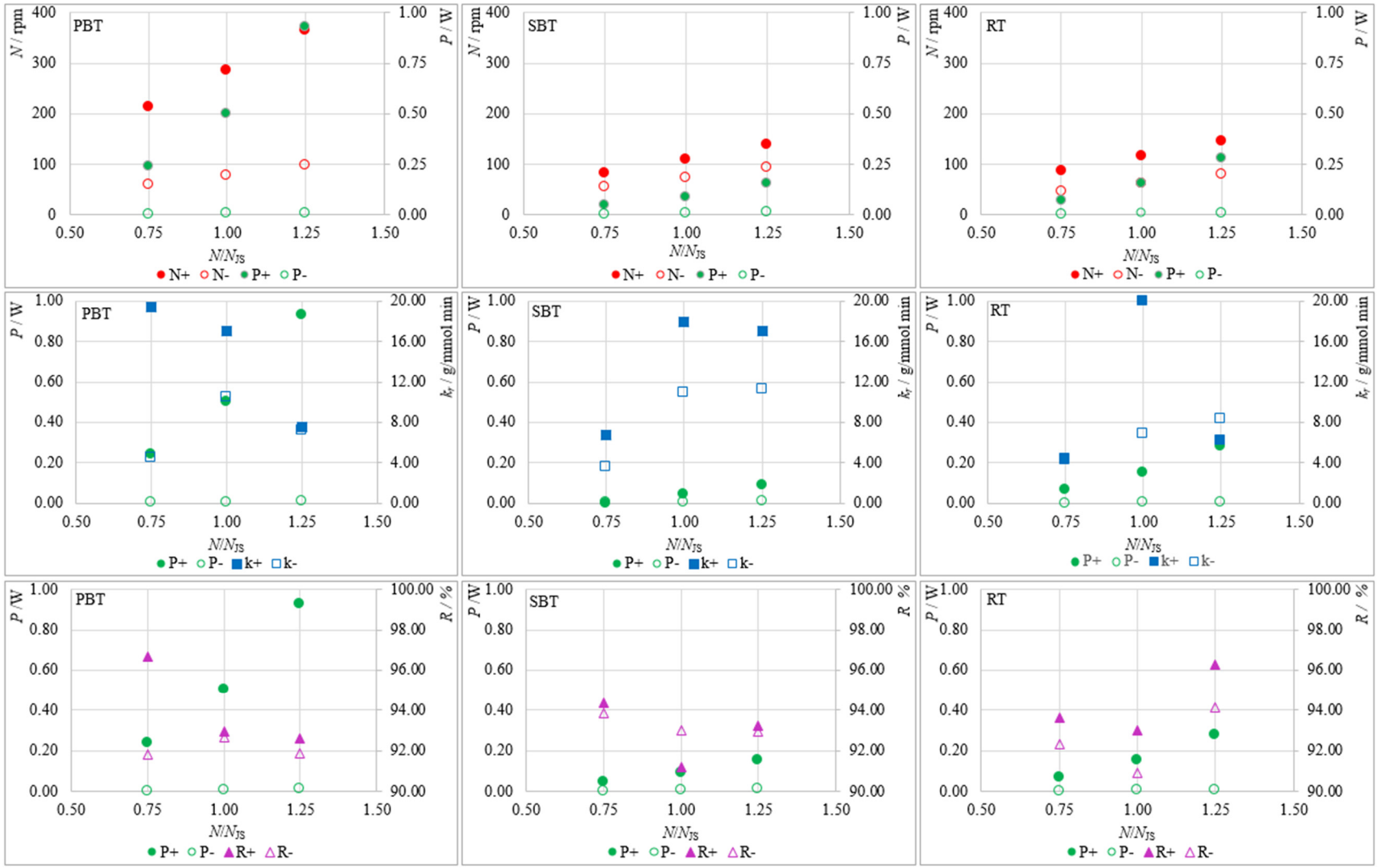


Figure 7. Changes in impeller speed, power consumption, rate constant and removal efficiency depending on N/N_{JS} for different types of impellers (+: baffled reactor; −: unbaffled reactor).

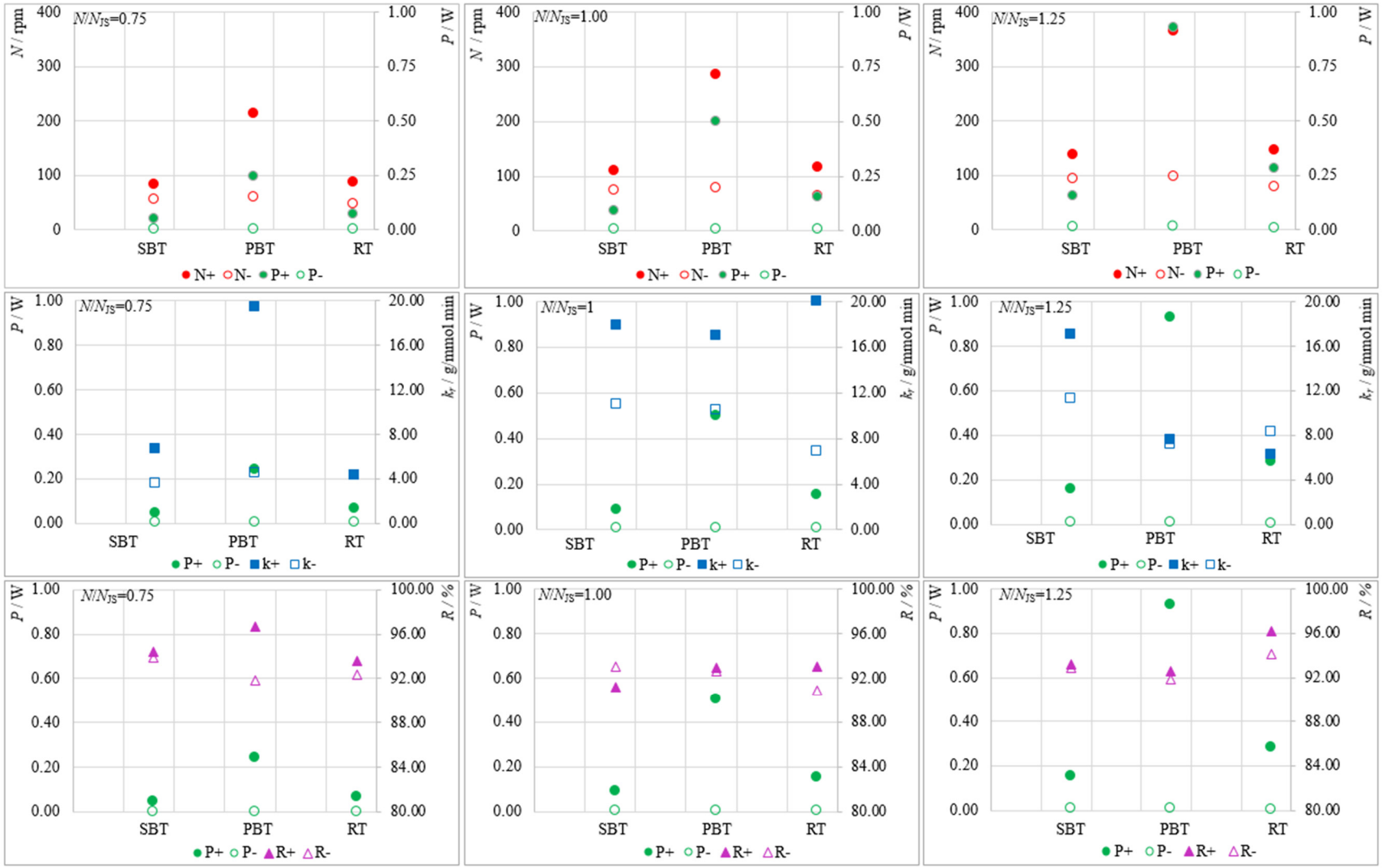


Figure 8. Changes in impeller speed, power consumption, rate constant and removal efficiency depending on the type of impeller for different N/N_{JS} (+: baffled reactor; −: unbaffled reactor).

The FTIR spectra of zeolite NaX, prior to and after the sorption process are plotted in Figure 9. The sorption process did not cause the degradation of the zeolite structure, since the recorded spectra before and after the sorption are almost identical. The bands recorded are the ones characteristic of the zeolite NaX.

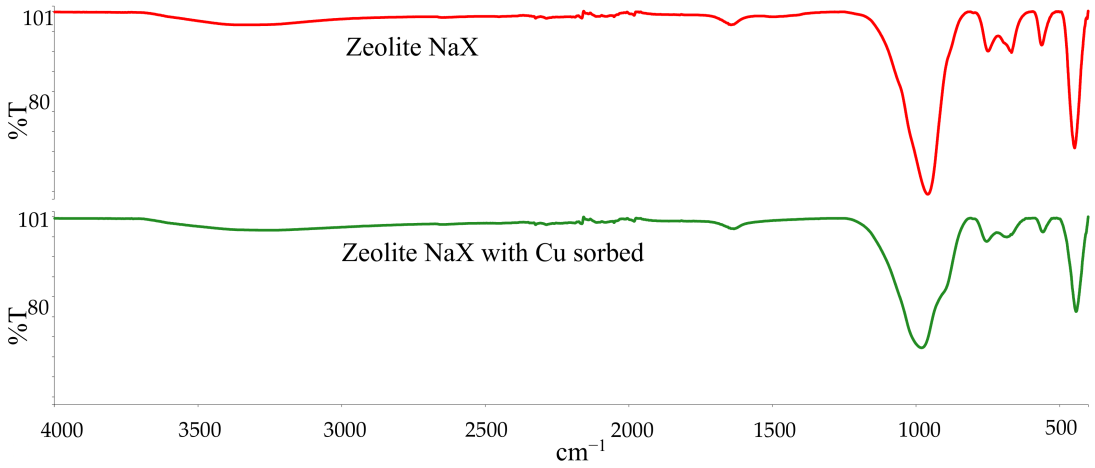


Figure 9. FTIR spectra of zeolite NaX, prior, and after the sorption process occurred.

4. Conclusions

The batch sorption process is widely employed for removing contaminants from wastewater and can be optimised by carefully selecting process parameters and reactor configurations. CFD has become one of the tools for chemical engineers enabling precise simulations of complex fluid flow phenomena. By optimising reactor designs, CFD can significantly reduce energy consumption and operational costs associated, among others, with wastewater treatment plants. Scaling may significantly affect transport phenomena and kinetics in the reactor. CFD is an effective method for assessing those changes and minimising potential risks.

This study investigates how reactor geometry and mixing speed, which are related to the suspension state, influence sorption kinetics and overall efficiency. It is found that the analysed process follows second-order kinetics. In most cases, the ψ parameter of the Mixed kinetic model is equal to zero or its value is slightly higher, indicating that diffusion has no effect on the kinetics of copper ion removal on zeolite and that all N/N_{JS} ratios applied ensure effective mixing. The amount of copper sorbed increases sharply in the initial phase of the process and then gradually increases until equilibrium is reached for all hydrodynamic conditions studied. The presence of baffles leads to an increase in critical speed for all impellers used. This is particularly pronounced for the PBT impeller, which is accompanied by the aeration in the system. Due to the proximity of the blades and the baffle plate/reactor wall, none of the impellers used generated the expected liquid flow. From an energy consumption perspective, reactors without baffles are a significantly better solution than baffled reactors, especially when using a PBT impeller. In unbaffled reactors, energy consumption differences are notably smaller, regarding the impeller type or mixing speed. From a kinetic standpoint, the best results are achieved at the highest N/N_{JS} or N_{JS}. The difference in rate constants between N/N_{JS} = 1.00 and 1.25 is smaller than for N/N_{JS} = 1.00 and 0.75. In baffled reactors, the SBT impeller proves to be the most efficient choice considering power consumption and process duration. Considering the compromises between power consumption and process duration the choice of reactor geometry and specific operating conditions should align with process priorities, such as energy savings through lower power consumption or reduced mixing time. The FTIR analysis confirms

that the sorbent structure remains intact after the sorption process, validating its long-term applicability.

Author Contributions: Conceptualisation, A.B., M.N.M. and S.S.; methodology, A.B., M.N.M., Ž.P. and S.S.; validation, A.B., M.N.M., Ž.P. and S.S.; formal analysis, A.B., M.N.M., Ž.P. and S.S.; investigation, A.B., M.N.M., Ž.P. and S.S.; resources, M.N.M., Ž.P. and S.S.; writing-original draft preparation, A.B., M.N.M. and S.S.; writing—review and editing, A.B., M.N.M., Ž.P. and S.S. All authors have read and agreed to the published version of the manuscript.

Funding: This research received no external funding.

Data Availability Statement: All the data are provided in the article already.

Acknowledgments: We are thankful for the scientific research equipment financed by EU grant, Functional integration of the University of Split, PMF-ST, PFST and KTFST through the development of the scientific and research infrastructure (KK.01.1.1.02.0018, and the project STIM–REI (contract number: KK.01.1.1.01.0003), funded by the European Union through the European Regional Development Fund—the Operational Programme Competitiveness and Cohesion 2014–2020 (KK.01.1.1.01.).

Conflicts of Interest: The authors declare no conflicts of interest.

References

1. Zlati, M.L.; Georgescu, L.P.; Iticescu, C.; Ionescu, R.V.; Antohi, V.M. New Approach to Modelling the Impact of Heavy Metals on the European Union's Water Resources. *Int. J. Environ. Res. Public Health* **2023**, *20*, 45. [CrossRef] [PubMed]
2. Raji, Z.; Karim, A.; Karam, A.; Khalloufi, S. Adsorption of Heavy Metals: Mechanisms, Kinetics, and Applications of Various Adsorbents in Wastewater Remediation—A Review. *Waste* **2023**, *1*, 775–805. [CrossRef]
3. Dichiara, A.B.; Weinstein, S.J.; Rogers, R.E. On the Choice of Batch or Fixed Bed Adsorption Processes for Wastewater Treatment. *Ind. Eng. Chem. Res.* **2015**, *54*, 8579–8586. [CrossRef]
4. Derbe, T.; Temesgen, S.; Bitew, M. A Short Review on Synthesis, Characterization, and Applications of Zeolites. *Adv. Mater. Sci. Eng.* **2021**, *2021*, 6637898. [CrossRef]
5. Castro, C.J.; Shyu, H.Y.; Xaba, L.; Bair, R.; Yeh, D.H. Performance and onsite regeneration of natural zeolite for ammonium removal in a field-scale non-sewered sanitation system. *Sci. Total Environ.* **2021**, *776*, 145938. [CrossRef]
6. Ezzedine, Z.; Batonneau-Gener, I.; Pouilloux, Y.; Hamad, H.; Saad, Z. Synthetic Nax Zeolite as a Very Efficient Heavy Metals Sorbent in Batch and Dynamic Conditions. *Colloids Interfaces* **2018**, *2*, 22. [CrossRef]
7. He, W.; Gong, H.; Fang, K.; Peng, F.; Wang, K. Revealing the effect of preparation parameters on zeolite adsorption performance for low and medium concentrations of ammonium. *J. Environ. Sci.* **2019**, *85*, 177–188. [CrossRef] [PubMed]
8. Jafari, R.; Tanguy, P.A.; Chaouki, J. Characterization of minimum impeller speed for suspension of solids in liquid at high solid concentration, using gamma-ray densitometry. *Int. J. Chem. Eng.* **2012**, *2012*, 945314. [CrossRef]
9. Zahoor, M. Effect of Agitation Speed on Adsorption of Imidacloprid on Activated Carbon. *J. Chem. Soc. Pak.* **2011**, *33*, 305–312.
10. Tamburini, A.; Brucato, A.; Cipollina, A.; Micale, G.; Ciofalo, M. CFD Predictions of Sufficient Suspension Conditions in Solid-Liquid Agitated Tanks. *Int. J. Nonlinear Sci. Numer. Simul.* **2012**, *13*, 427–443. [CrossRef]
11. Bašić, A.; Penga, Ž.; Penga, J.; Kuzmanić, N.; Svilović, S. Zeolite NaX Mass and Propeller Agitator Speed Impact on Copper Ions Sorption. *Processes* **2023**, *11*, 264. [CrossRef]
12. Bašić, A.; Svilović, S. Effect of geometrical and operating mixing parameters on copper adsorption on zeolite NaX. *Desalin. Water Treat.* **2021**, *209*, 197–203. [CrossRef]
13. Svilović, S.; Smajo, I.; Stipišić, R.; Rušić, D.; Kuzmanić, N. Utjecaj brzine vrtnje SBT miješala na kinetiku izmjene bakra na zeolitu—Impact of impeller speed on copper exchange kinetics on zeolite. In Proceedings of the International Conference MATRIB 2016, Materials, Tribology, Recycling, Vela Luka, Korčula, Croatia, 23–25 June 2016.
14. Lodh, B.K. The transformative role of Computational Fluid Dynamics (CFD) in chemical engineering. *Open J. Chem.* **2024**, *10*, 1–3. [CrossRef]
15. Ranade, V.V. *Computational Flow Modeling for Chemical Reactor Engineering*, 1st ed.; Academic Press: Cambridge, MA, USA, 2001; Volume 5, pp. 286–323.
16. Bullen, J.C.; Saleesongsom, S.; Gallagher, K.; Weiss, D.J. A Revised Pseudo-Second-Order Kinetic Model for Adsorption, Sensitive to Changes in Adsorbate and Adsorbent Concentrations. *Langmuir* **2021**, *37*, 3189–3201. [CrossRef]
17. Sadeek, S.A.; Negm, N.A.; Hefni, H.H.H.; Wahab, M.M.A. Metal adsorption by agricultural biosorbents: Adsorption isotherm, kinetic and biosorbents chemical structures. *Int. J. Biol. Macromol.* **2015**, *81*, 400–409. [CrossRef]

18. Weber, W.J. Evolution of a technology. *J. Environ. Eng.* **1984**, *110*, 899–917. [CrossRef]
19. Haerifar, M.; Azizian, S. Mixed surface reaction and diffusion-controlled kinetic model for adsorption at the solid/solution interface. *J. Phys. Chem. C* **2013**, *117*, 8310–8317. [CrossRef]
20. Tran, H.N.; You, S.-J.; Hosseini-Bandegharaei, A.; Chao, H.-P. Mistakes and inconsistencies regarding adsorption of contaminants from aqueous solutions: A critical review. *Water Res.* **2017**, *120*, 88–116. [CrossRef]
21. Wang, J.; Guo, X. Adsorption kinetic models: Physical meanings, applications, and solving methods. *J. Hazard. Mater.* **2020**, *390*, 122156. [CrossRef]
22. Yao, C.; Chen, T. A film-diffusion-based adsorption kinetic equation and its application. *Chem. Eng. Res. Des.* **2017**, *119*, 87–92. [CrossRef]
23. Blanchard, G.; Maunaye, M.; Martin, G. Removal of heavy metals from waters by means of natural zeolites. *Water Res.* **1984**, *18*, 1501–1507. [CrossRef]
24. Lisbania Velarde, L.; Nabavi, M.S.; Escalera, E.; Antti, M.-L.; Akhtar, F. Adsorption of heavy metals on natural zeolites: A review. *Chemosphere* **2023**, *328*, 138508. [CrossRef] [PubMed]
25. Zwietering, T. Suspending of solid particles in liquid by agitatiors. *Chem. Eng. Sci.* **1958**, *8*, 244–253. [CrossRef]
26. Bašić, A.; Mužek, M.N.; Svilović, S. Influence of impeller clearance, impeller size and baffles on copper sorption on zeolite NaX: Do the size and position really matter? *Appl. Surf. Sci. Adv.* **2023**, *18*, 100507. [CrossRef]
27. Ritchie, A.G. Alternative to Elovich equation for the kinetics of adsorption of gasses on solids. *J. Chem. Soc. Faraday Trans. 1* **1977**, *73*, 1650–1653. [CrossRef]
28. Bašić, A.; Penga, Ž.; Mužek, M.N.; Svilović, S. Impact of turbine impeller blade inclination on the batch sorption process. *Results Eng.* **2022**, *16*, 100554. [CrossRef]
29. Tamburini, A.; Cipollina, A.; Micale, G.; Brucato, A. Measurements of Njs and Power Requirements in Unbaffled Bioslurry Reactors. *Chem. Eng. Trans.* **2012**, *27*, 343–348. [CrossRef]
30. Cohen, B.M.; Inankur, B.; Lauser, K.T.; Lott, J.; Chen, W. Evaluation of Just-Suspended Speed Correlations in Lab-Scale Tanks with Varying Baffle Configurations. *Org. Process Res. Dev.* **2018**, *22*, 1481–1488. [CrossRef]
31. Glover, G.M.C.; Fitzpatrick, J.J. Modelling vortex formation in an unbaffled stirred tank reactors. *Chem. Eng. J.* **2007**, *127*, 11–22. [CrossRef]
32. Raghava Rao, K.S.M.S.; Rewatkar, V.B.; Joshi, J.B. Critical impeller speed for solid suspension in mechanically agitated contactors. *AIChE J.* **1988**, *34*, 1332–1340. [CrossRef]
33. Svilović, S.; Horvat, I.; Ćosić, M.; Stipišić, R. Investigation on the effects of process variables on copper exchange on NaX in a batch stirred reactor. *Teh. Glas.* **2017**, *11*, 171–174. Available online: https://hrcak.srce.hr/190995 (accessed on 16 December 2024).
34. Uehara-Nagamine, E. Solids Suspension and Power Dissipation in Stirred Tanks Agitated by an Impeller near the Tank Bottom. Ph.D. Thesis, New Jersey Institute of Technology, Newark, NJ, USA, 31 October 1996. Available online: https://digitalcommons.njit.edu/theses/1071 (accessed on 16 December 2024).
35. Tsui, Y.-Y.; Lin, S.-C.; Shen, S.-J.; Hu, Y.-C. Analysis of the flow agitated by disc impellers with pitched blades. *Numer. Heat Transf. A Appl.* **2008**, *53*, 1091–1108. [CrossRef]
36. Kresta, S.M.; Wood, P.E. The mean flow field produced by a 45° pitched blade turbine: Changes in the circulation pattern due to bottom clearance. *Can. J. Chem. Eng.* **1993**, *71*, 42–53. [CrossRef]
37. Brucato, A.; Cipollina, A.; Micale, G.; Scargiali, F.; Tamburini, A. Particle suspension in top-covered unbaffled tanks. *Chem. Eng. Sci.* **2010**, *65*, 3001–3008. [CrossRef]
38. Ameur, H.; Kamla, Y.; Sahel, D. CFD Simulations of Mixing Characteristics of Radial Impellers in Cylindrical Reactors. *ChemistrySelect* **2016**, *1*, 2548–2551. [CrossRef]

Disclaimer/Publisher's Note: The statements, opinions and data contained in all publications are solely those of the individual author(s) and contributor(s) and not of MDPI and/or the editor(s). MDPI and/or the editor(s) disclaim responsibility for any injury to people or property resulting from any ideas, methods, instructions or products referred to in the content.